Article

Not peer-reviewed version

Optical Properties of Composite Silver Nanoparticles

Ibrahim Elagib Ali * and Wafa Sultan Almutairi

Posted Date: 25 January 2023

doi: 10.20944/preprints202301.0453.v1

Keywords: Arabic gum; nanocomposite; melanin; optical properties; silver nanoparticles

Article

Optical Properties of Composite Silver Nanoparticles

Wafa Sultan Almutairi[1] and IIbrahim Elagib Ali [1,*]

1 Physics & Astronomy Department, College of Science, King Saud University, P.O. Box 2455, Riyadh 11451, Saudi Arabia
* Correspondence: elagibali@ksu.edu.sa

Abstract: Composite silver nanoparticles were synthesised using melanin broth and Arabic gum as a reducing and binding agent. The reactions are carried out with water because it is a non-hazardous solvent. The produced composites either had specified diameters (average diameter of 50 nm) with high silver loading or lower loading composites with tuneable morphologies and electrical properties. UV-IR, gamma, and conventional light are used to characterise the synthesised composite silver nanoparticles. Furthermore, measurements are carried out of the dielectric constant, refractive index, energy gap, optical and electrical conductivities, and refractive index coefficients. The silver nanoparticle formation was validated by UV-Vis measurement of the sample, which demonstrated a distinct peak at a wavelength of 420 nm. The characteristics of the composite silver nanoparticles are also quantified using several methods, including XRD, SEM, and particle size analysis.

Keywords: Arabic gum; nanocomposite; melanin; optical properties; silver nanoparticles

1. Introduction

Nanotechnology is defined as the manipulation of single atoms and molecules having a size of fewer than 100 nanometers [1]. Richard Feynman coined the word "nanotechnology," and it was first used in scientific circles in 1974 [2]. Nanoparticles are used in catalysis, electronic devices, dyes, and pigments, among other things [3,4]. For centuries, silver-based compounds have been employed as harmless inorganic antibacterial agents in a variety of applications for millennia. Because of their biocidal qualities, including wood preservatives, water purification in hospitals, wound or burn care, and so on. Silver ions and similar compounds have modest toxicity to animal cells but significant toxicity to microorganisms such as bacteria and fungi [5].

Due to their distinctive physical and chemical properties, silver nanoparticles (AgNPs) are increasingly used in a variety of industries, including medicine, food, health care, consumer goods, and industry. Optical, electrical, and thermal properties, as well as high electrical conductivity and biological properties, are among them [6–8].

These nanoparticles have been used as antibacterial agents, in the industrial, household, and healthcare-related products, in consumer products, medical device coatings, optical sensors, and cosmetics, in the pharmaceutical and food industries; in diagnostics, orthopedics, drug delivery, and as anticancer agents, and have ultimately enhanced the tumor-killing effects of anticancer drugs [9]. The silver nanoparticle research continues to grow, drawing the attention of researchers. It is known that silver has very high electrical conductivity [10,11]. Silver has been widely used as a conductor wire in circuits that require low dissipation, and high conductivity [12,13]. Silver paste has also been widely used as a paste conductor [14,15]. The use of silver paste has been extensively utilized mainly in the bulk conductivity characterization of bulk semiconductor materials or four-point probe method films. In the field of superconductors, silver has a dominant role as a sheath [16–18]. Silver has also been used in various industries and health fields. Silver is known to have antibacterial properties [4,6,16,19,20], as a catalyst [21], and it shows stability to the environment [22] and has been utilized as a significant component of water treatment.

Various methods of synthesis have been developed to produce silver nanoparticles. The synthesis of the silver nanoparticle is commonly known to control the shape and size. Among these

Preprints.org (www.preprints.org) | NOT PEER-REVIEWED | Posted: 25 January 2023 doi:10.20944/preprints202301.0453.v1

methods are the ball milling method [23], precipitation, polyol method, and several other methods to produce silver nanoparticles [12,24,25]. AgNPs have recently been popular in a variety of fabrics, keyboards, wound dressings, and biomedical devices [7,26,27]. In chemistry and chemical technology, environmentally friendly synthesis processes are becoming increasingly prominent. This tendency may be traced back to numerous factors, including the need for greener solutions to offset the increased prices and energy demands of physical and chemical processes. As a result, scientists are looking for less expensive synthesis methods. The other reason is that traditional nanoparticle synthesis methods typically need dangerous reductants like sodium borohydride or hydrazine, as well as numerous steps in the synthesis process, including heat treatments, which sometimes result in hazardous by-products. Greener techniques for nanoparticle synthesis have been researched for over a decade to lessen the environmental impact of nanoparticle synthesis. Anastas and Warner proposed the concepts of green chemistry, which they refined into 12 principles that eloquently characterize green chemistry [28]. The synthesis steps should be carried out at near to ambient temperature and pressure, with a neutral pH, to save energy. Biological systems appear to be the best factory for achieving these natural chemical conditions. Many microorganisms may produce inorganic materials either intracellularly or extracellularly [29], and it has been discovered that certain of these microbes can be exploited as environmentally friendly nano-factories for the manufacture of nanomaterials, particularly silver metal nanoparticles (Ag NPs).

Interestingly, biologically-prepared AgNPs show high yield, solubility, and high stability [30]. Among several synthetic methods for AgNPs, biological methods seem to be simple, rapid, non-toxic, dependable, and green approaches that can produce well-defined size and morphology under optimized conditions for translational research. In the end, a green chemistry approach for the synthesis of AgNPs shows much promise. Studies on the electrical and optical properties of polymers have gotten a lot of attention in recent years because of their use in electronic and optical devices. Electrical conduction in polymers has been investigated to better understand the nature of charge transport in these materials, while optical characteristics have been improved to improve reflection, antireflection, interference, and polarization. Depending on their reactivity with the host matrix, dopants can be used to modify the electrical and optical properties of polymers. Although considerable research on charge carrier transport and optical characteristics of doped polymers has been published [31–37].

Ionizing radiation is a type of energy that removes electrons from atoms and molecules in a variety of materials, including air, water, and living tissue. Ionizing radiation can flow through these materials undetected [38,39]. X-rays, which may enter our bodies and expose images of our bones, are a common example of ionizing radiation. X-rays are called "ionizing" because they have the unique capacity to take electrons from atoms and molecules in the substance they pass through. Ionizing radiation includes the more energetic end of the electromagnetic spectrum (ultraviolet, X-rays, and gamma rays) and subatomic particles, such as electrons, neutrons, and alpha particles (helium nuclei each comprising two protons and two neutrons). Ionizing activity can change molecules within our body's cells. That action could affect us in the long run (such as cancer). Ionizing radiation exposures that are too intense might cause skin or tissue damage [40,41]. The boundary between ionizing and non-ionizing radiation in the ultraviolet area is not sharply defined because different molecules and atoms ionize at different energies. The energy of ionizing radiation starts between 10 (eV) and 33 eV and extends further up. An instrument like the Geiger counter can detect such radiations.

In this research $AgNO_3$ nanoparticles are prepared with different concentrations with the addition of 0.50 g of Arabic Gum at a temperature of 200 °C and melanin broth at temperature 4 °C is added to the $AgNO_3$ solution of different molarity at a temperature of 200 °C. Several solutions with different concentrations are prepared. The melanin is synthesized from defatted Nigella Sativa processed by ethylene. For optical properties, a wavelength ranging from 200 to 800 nm is used to irradiate the prepared sample (AgO nanoparticles). Two peaks were observed. One is attributed to the presence of melanin because the melanin has a high ability to absorb UV and the other peak is attributed to the presence of silver oxide nanoparticles and according to literature [42,43]. The former is very sharp while the latter is rather shallow. Other optical and electric conductivity properties are calculated by plotting different behavior of the sample with light wavelengths.

2. Experiments

2.1. Preparation of composite silver nanoparticles

In this study, we will show the method and preparation of $AgNO_3$ mixed with melanin broth and Arabic Gum with the aid of distilled water under different concentrations of silver nitrate as shown in Table 1. Silver nitrate is an inorganic compound with the chemical formula $AgNO_3$. In its solid form, silver nitrate is coordinated in a trigonal planar arrangement. It is often used as a precursor to other silver-containing compounds. It is used in making photographic films, and in laboratory setting as a staining agent in protein visualization in PAGE gels. There are two types of melanin, one is natural and the other is synthetic. The natural one is extracted from Nigella Sativa seeds after taking off oil using a simple chemical process. The synthetic melanin is purchased from Sigma-Aldrich. The Gum Arabic is a natural gum consisting of the hardened sap of two species of the acacia (sensu lato) tree, Senegalia senegal and Vachellia seyal. Gum Arabic's mixture of polysaccharides and glycoproteins gives it the properties of a glue and binder that is edible by humans. Its use here is to help regimenting nanoparticles in rounded forms. Gum Arabic quickly dissolves in water to give clear solutions ranging in color from very pale yellow to orange-brown and with a pH of ~ 4.5.

In this method, we intend to prepare nanoparticles from 18 samples containing 100 ml of distilled water in all cases 0.5 g of Arabic Gum is added to $AgNO_3$ solutions with different concentrations (0.1 g to 2.75g) all being heated at 200 ˚C. 50 ml melanin broth are added to the solution drop wise until a formation of the color of the solution turns to orange that indication of silver nanoparticles was synthesized.

Table 1. Formulation of composite samples preparation.

S.No.	$AgNo_3$ (g)	DW(distilled water) (ml)	200 °C 0.5 g AG	MB(melanin broth)
S1	0.050	100 ml	0.5	50 ml
S2	0.100	100 ml	0.5	50 ml
S3	0.150	100 ml	0.5	50 ml
S4	0.3	100 ml	0.5	50 ml
S5	0.4	100 ml	0.5	50 ml
S6	0.5	100 ml	0.5	50 ml
S7	0.6	100 ml	0.5	50 ml
S8	0.7	100 ml	0.5	50 ml
S9	0.8	100 ml	0.5	50 ml
S10	0.9	100 ml	0.5	50 ml
S11	1.0	100 ml	0.5	50 ml
S12	1.25	100 ml	0.5	50 ml
S13	1.5	100 ml	0.5	50 ml
S14	1.75	100 ml	0.5	50 ml
S15	2 .0	100 ml	0.5	50 ml
S16	2.25	100 ml	0.5	50 ml
S17	2.50	100 ml	0.5	50 ml
S18	2.75	100 ml	0.5	50 ml

2.2. Analyzing techniques for composite silver nanoparticles

Shimadzu Double Beam Double Monochromator Spectrophotometer (UV-2550) equipped with an Integrating Sphere Assembly ISR-240A in the wavelength range of 200-800 nm with a resolution of 0.5 nm was utilized to record the absorption and reflection spectra of composite Ag particles. The absorption spectra of colloidal solution of composite was recorded by taking distilled water as reference. From these spectra various optical constants such as optical energy gap, and optical conductivity were determined. The produced composite samples were subjected to X-ray diffraction experiments using a JEOL JDX-8P-X-ray diffractometer with Cu-Kα radiation in the diffraction angle (2θ) range of 10° to 80°. X-ray tube operation parameters were 40 kV and 30 mA. In order to evaluate the morphology of the composite materials, pictures of the surface texture were examined using scanning electron microscopy (SEM, JEOL, Japan). Samples were attached to sample holders (also known as specimen stubs) for the SEM evaluation using conductive double-sided carbon tape. In order to render the samples electrically conducive, they were subsequently put in a vacuum chamber for platinum sputtering. The surface morphology of the composite material samples was examined using a 5 kV acceleration voltage. A Zetasizer Nano Instrument (Malvern Instruments, Nano ZS, ZEN3600, UK) employing a 532 nm laser was utilised to measure the particle size distribution of the powdered composite materials sample. The nanoparticle powder sample was dispersed in milli Q water by horn type ultrasonic processor (Vibronics, model: VPLP1) generating a total concentration of 1% at 37 ° c in order to determine the particle size distribution.

3. Results and Discussions

3.1. Particle size of composite silver nanoparticles

The Dynamic Light Scattering (DLS) analytical approach quantifies the Brownian motion of composite nanoparticles. DLS is one of the most significant and helpful techniques for evaluating particle size and size distribution of prepared composite nanomaterial in solution. DLS uses a laser beam to illuminate a particle that is moving according to Brownian motion to determine the size of colloidal dispersions. The results of such analysis are shown in Figure 2. Due to the hydrodynamic size of nanomaterials, the DLS pattern showed that the produced composite Ag nanoparticles had an average size of 50±15 nm. Numerous variables, such as pH, precursor concentration, reductant concentration, incubation duration, temperature, and production process, have an impact on the shapes and sizes of metal nanoparticles.

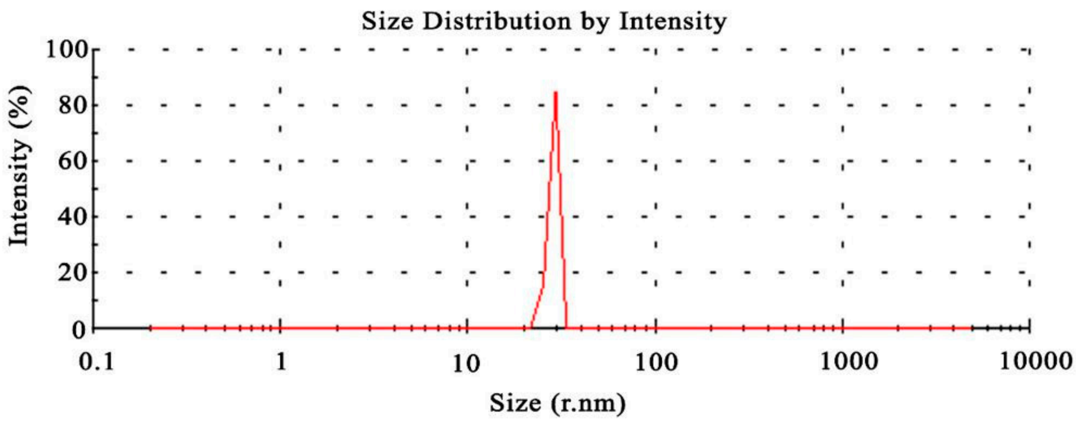

Figure 1. Dynamic light scattering analysis of the particle size distribution of the composite silver nanoparticles.

3.2. Morphology of composite silver nanoparticles

Scanning electron microscopy was used to analyse the surface morphology of the produced composite silver nanoparticles and shows in Figure 3. The SEM images of Arabic gum and melanin broth with a surface of silver on them are shown in Figures 3b-d. The concentration of the AgNO3 applied in these images reveals a proportional improvement in the amount of silver in the composite matrix. It was shown that relatively spherical and uniform Ag nanoparticles were formed with

Preprints.org (www.preprints.org) | NOT PEER-REVIEWED | Posted: 25 January 2023 doi:10.20944/preprints202301.0453.v1

diameter of 53 to 150 nm. The homogeneity and distribution of the AgNPs with melanin broth and Arabic Gum composite surface are quite similar to other synthesis methods; this was possible because experimental conditions allowed controlling the amount of deposited particles, and thus, the formation of agglomerates that increase the density of the solids. The appearance of the particles, as per the analysis, was highly crystalline and spherical in shape. An investigation of some larger composite nanoparticles attributed to the fact that silver nanoparticles had the ability to agglomerate due to their high surface energy. In nanometer scale, some of the silver nanoparticles contributed to grow into twinned particles. Figure 3e shows the representative SEM micrographs of the composites silver nanoparticles. It is shown that all silver nanoparticles are spherical. These results demonstrate good agreement with the PSD single peak results obtained in Figure 2. The diameter particle of the particles in the composite sample is 45±9.55 nm over the counted 46 particles.

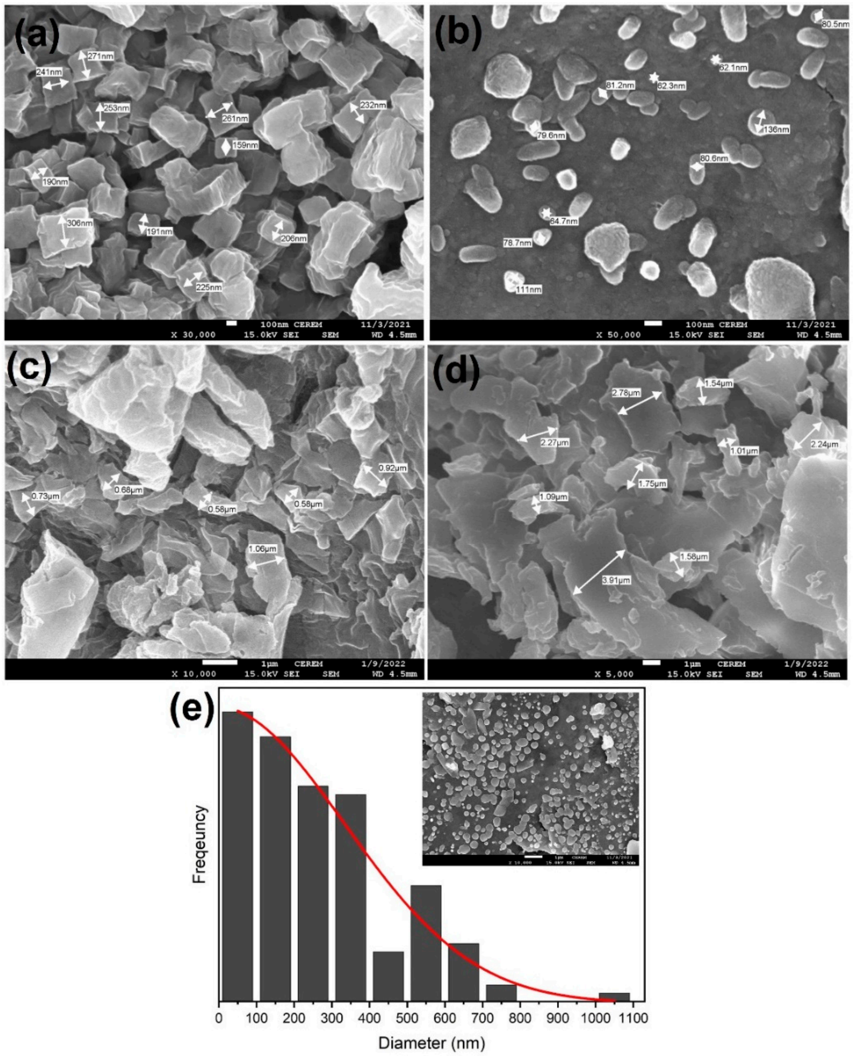

Figure 2. SEM image for composite silver nanoparticles.

3.3. Spectral properties of composite silver nanoparticles

The X-ray diffraction was performed for the solution silver nanoparticles. In the X-ray diffractogram of $AgNO_3$ with a concentration 0.3g, one sharp diffraction peak was revealed at diffraction angle 34° (Figure 4a). It can be shown that when the $AgNO_3$ concentration 0.7g, two sharp diffraction peaks were depicted at 34° and 44°, as shown in Figure 4b. Another sample of concentration with 1.25g has three sharp peaks at angles of 34°, 44° and 56° (Figure 4c). A fourth

 doi:10.20944/preprints202301.0453.v1

sample whose concentration with 2.25g shows the four sharp diffraction peaks at angles of 34°, 44°, 56° and 75° (Figure 4d). This diffractogram showed the crystalline nature of $AgNO_3$. The same diffraction peaks revealed in the physical mixture pattern by reduction of intensity. This diffraction indicated that $AgNO_3$ was presented as an amorphous material.

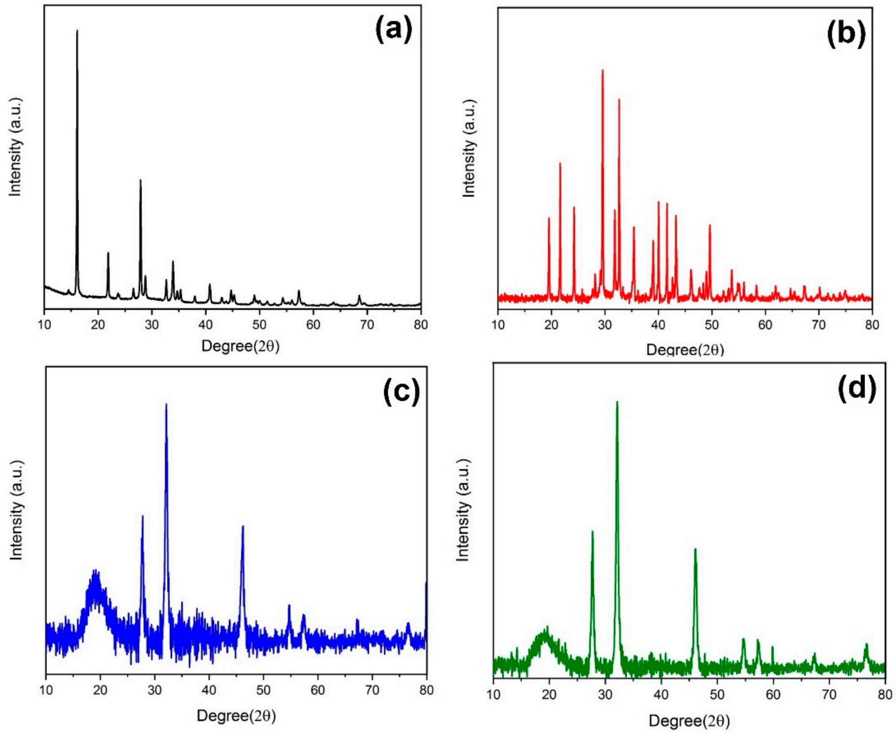

Figure 3. X-ray diffraction patterns of composite material decorated by different Ag nanoparticles amount (a) 0.3g, (b) 0.7g (c) 1.25g,and 2.25g.

3.4. Optical absorbance and absorption coefficient of composite silver nanoparticles

Figure 5 illustrates the absorption spectra of the composite samples that were obtained from the dispersion of various amounts of $AgNO_3$ into constant melanin broth (50 ml) and Arabic Gum 0.5 g solution in order to investigate the effects of melanin broth and Arabic Gum on the optical properties of Ag nanoparticles. Except for melanin broth and Arabic gum, the absorption spectra of these substances clearly exhibit bimodal features, with a narrow peak in the visible region resulting from the adsorption of silver nanoparticles in the UV region, which corresponds to the fundamental absorption of the surfaces of melanin broth and Arabic gum. The wavelengths of the maximum absorbance moved from 415 to 450 nm, as shown in the absorption spectra. According to the quantum theory of metal nanoparticles, the maximum absorbance wavelength is related to the energy of the conduction band. After 450 nm, there are no peaks to be found, suggesting that there has been no agglomeration of nanoparticles. According to figures, there is a noticeable improvement in the band's intensity as the concentration of silver nitrate increases. This shows that there has been an increase in the generation of silver nanoparticles in the Arabic Gum and Melanin solution. The typical UV-Vis absorption spectra of the resultant solutions are displayed that following concentrations of solutions were oxidised with silver nitrate at a temperature of 200 °C.

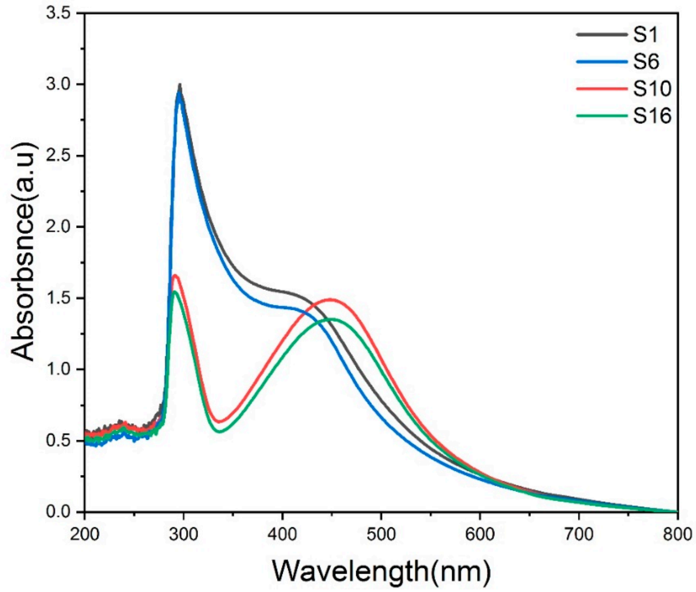

Figure 4. Variation of optical absorption with wavelength for composite films containing different Ag nanoparticle amount.

3.5. Optical conductivity of composite silver nanoparticles

The optical conductivity of nanoparticles is among their most significant and unique properties. The terminology of optical conductivity refers to the movement of charge carriers caused by the alternating electric field of the incident electromagnetic waves. Figure 6 illustrates the wavelength dependency of the optical absorbance of Ag nanoparticles functionalized with Arabic gum and melanin in the wavelength range of 200–800 nm. For composite products manufactured of Arabic gum, melanin, and $AgNO_3$, figure depicts how optical conductivity changes with wavelength. According to the results, composite films have the ability to absorb light across a broad spectrum range because the absorbance spectra appear to have the same shape and tend to increase as Ag nanoparticle concentration increases. The finding suggests that the optical conductivity improves as the concentration of Ag nanoparticles increases. This rise may be caused by the development of new levels in the energy gap, which allows electrons to transfer from the valence band to the conduction band via these new levels, resulting in a decrease in the energy gap and an increase in optical conductivity. The optical conductivity is increasing, which means that the electrons are absorbing incident photons at a higher rate for a given energy. When Ag nanoparticle concentration is greater, optical conductivity is greatest at the wavelength of surface plasmon resonance. Therefore, the combination of Ag nanoparticles with the matrix of Arabic gum and melanin induces the formation of trap states in the HOMO-LUMO gap. These phases cause the differences in optical energy gap, Urbach's energy, and optical conductivity that have been noticed. These findings could make it possible to modify the material's characteristics in anticipation of using Ag nanocomposite in a variety of real-world applications.

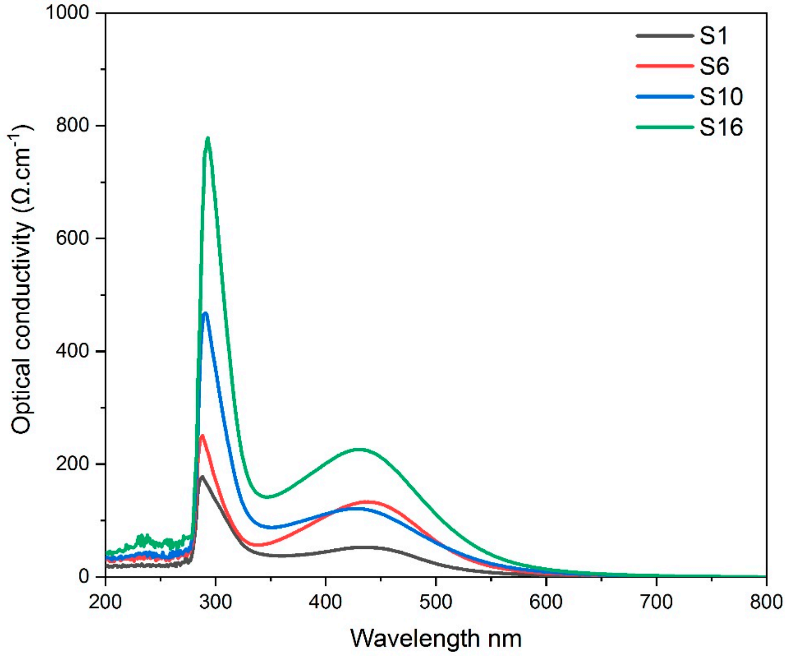

Figure 5. Variation of optical conductivity with wavelength for composite films containing different Ag nanoparticle amount.

3.6. Variation of refractive index of composite silver nanoparticles

Ag nanoparticles have exceptional optical characteristics that set them apart from bulk material. When composite Ag nanoparticles interact with incident light of a particular wavelength, a phenomenon known as localised surface plasmon resonance occurs. This phenomenon causes the local electric field surrounding the nanoparticles to be significantly increased, which in turn causes the nanoparticles to absorb and scatter light. Ag nanoparticle composites have several uses because of their unique optical characteristics. The change in refractive index of the surrounding medium has a significant impact on nanoparticle localised surface plasmon resonance. As a result, the incorporation of the shift in resonance wavelength may be used to assess changes in the nearby environment. The refractive index of composite Ag nanoparticles in an associated medium is shown in Figure 7 along with resonance wavelengths. As the ambient refractive index increases from 1.8 to 3.5, the resonance wavelength of composite matrix with different concentration of Ag nanoparticles shifts from 422 nm to 459 nm.

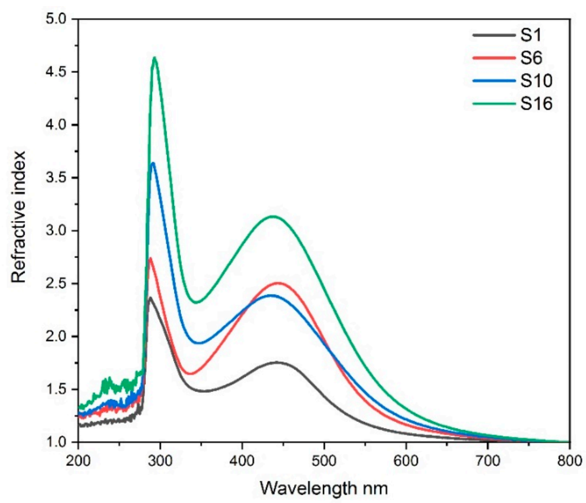

Figure 6. The refractive index of composite film decorated by different Ag nanoparticles with amount.

3.7. Band gap energy of composite silver nanoparticles

A composite material's band gap energy is the distance between the valence band and the lowest empty conduction band. It is a factor that determines how much photon energy must be absorbed by the materials to produce photoelectron and photoholes. The data acquired from the absorption spectra may be used to plot $(\alpha hv)^2(eV.cm^{-1})^2$ vs the eV using the absorption spectra, as illustrated in Figures 30 to 33. The results of the absorption spectra were utilised to calculate the band gap energy of each of the composite materials using Tauc graphs. It demonstrates that the plotted data provides tangent to the linear portion of the curves in a certain area. The band gap energy has been calculated for composite materials are (2.25 to 1.95 eV) for samples from S1 to S16. It is important to note that the reported band gap energy values are smaller than the band gap of lower amounts of Ag nanoparticles. Based on these findings, it may be concluded that band gap energy values drop as concentrations rise. This finding may be attributed to the optical confinement effect in accordance with the size and length of Ag nanoparticles based on the band gap energy of the composite materials.

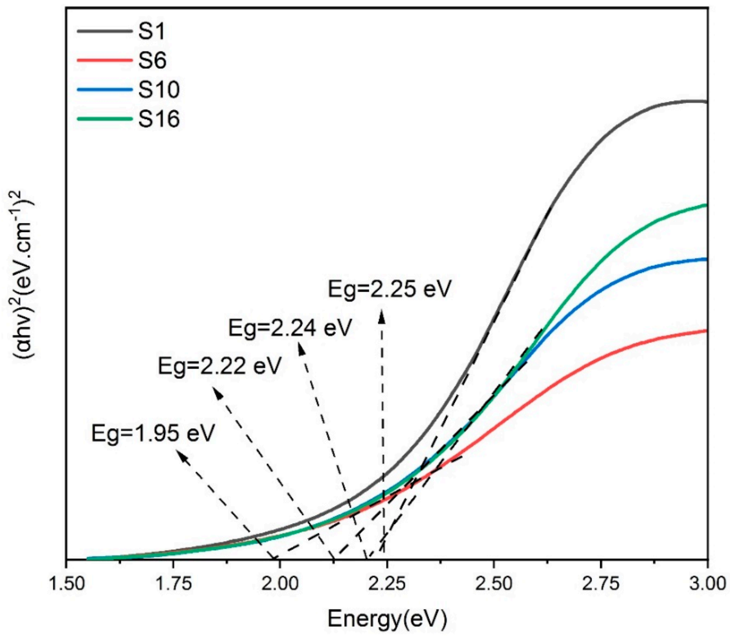

Figure 7. Tauc plots for the evaluation of band gap energy of composite film decorated by different Ag nanoparticles with the amount.

4. Conclusions

The area of electrical properties study, where nanotechnology is combined with the three scientific disciplines of physics, biology, and chemistry, is where the influence of nanotechnology is currently and potentially most visible. The usage of nanoparticles in electrical properties together with current research for easy regulated (morphological characteristics) development of composite nanoparticles is still a very active and growing topic for researchers. The composite silver nanoparticles were synthesised using melanin broth and Arabic gum as a reducing and binding agent. The reactions are carried out with water because it is a non-hazardous solvent. The synthesis of the composite silver nanoparticles at 200 °C temperatures, together with the usage of the reducing and binding agent, had a significantly positive influence on the uniformity of the generated structures, as measured by UV-Vis spectroscopy and Dynamic Light Scattering. The presence of silver nanoparticles was originally established by the absorbance spectra of the materials with the characteristic Plasmon band, the small peak of the band suggesting a confined particle size range.

The produced composites either had specified diameters (average diameter of 50 nm) with high silver loading or lower loading composites with tuneable morphologies and electrical properties. The electrical properties application of the composite silver nanocomposite was investigated

References

1. C. Dhand, N. Dwivedi, X.J. Loh, A.N. Jie Ying, N.K. Verma, R.W. Beuerman, R. Lakshminarayanan, S. Ramakrishna, Methods and strategies for the synthesis of diverse nanoparticles and their applications: a comprehensive overview, RSC Adv. 5 (2015) 105003–105037. https://doi.org/10.1039/C5RA19388E.
2. I. Ghiuță, D. Cristea, D. Munteanu, Synthesis Methods of Metallic Nanoparticles-an Overview, Bull. Transilv. Univ. Braşov. 10 (2017) 133–140. http://webbut.unitbv.ro/bulletin/Series I/2017/BULETIN I/Ghiuta_I.pdf.
3. X. Li, H. Xu, Z.S. Chen, G. Chen, Biosynthesis of nanoparticles by microorganisms and their applications, J. Nanomater. 2011 (2011). https://doi.org/10.1155/2011/270974.
4. I. Ban, J. Stergar, M. Drofenik, G. Ferk, D. Makovec, Synthesis of chromium-Nickel nanoparticles prepared by a microemulsion method and mechanical milling, Acta Chim. Slov. 60 (2013) 750–755.
5. H.J. Klasen, A historical review of the use of silver in the treatment of burns. II. Renewed interest for silver, Burns. 26 (2000) 131–138. https://doi.org/https://doi.org/10.1016/S0305-4179(99)00116-3.
6. S. Gurunathan, J.H. Park, J.W. Han, J.H. Kim, Comparative assessment of the apoptotic potential of silver nanoparticles synthesized by Bacillus tequilensis and Calocybe indica in MDA-MB-231 human breast cancer cells: Targeting p53 for anticancer therapy, Int. J. Nanomedicine. 10 (2015) 4203–4223. https://doi.org/10.2147/IJN.S83953.
7. W.-R. Li, X.-B. Xie, Q.-S. Shi, H.-Y. Zeng, Y.-S. OU-Yang, Y.-B. Chen, Antibacterial activity and mechanism of silver nanoparticles on Escherichia coli, Appl. Microbiol. Biotechnol. 85 (2010) 1115–1122. https://doi.org/10.1007/s00253-009-2159-5.
8. P. Mukherjee, A. Ahmad, D. Mandal, S. Senapati, S.R. Sainkar, M.I. Khan, R. Parishcha, P. V Ajaykumar, M. Alam, R. Kumar, M. Sastry, Fungus-Mediated Synthesis of Silver Nanoparticles and Their Immobilization in the Mycelial Matrix: A Novel Biological Approach to Nanoparticle Synthesis, Nano Lett. 1 (2001) 515–519. https://doi.org/10.1021/nl0155274.
9. S. Chernousova, M. Epple, Silver as Antibacterial Agent: Ion, Nanoparticle, and Metal, Angew. Chemie Int. Ed. 52 (2013) 1636–1653. https://doi.org/https://doi.org/10.1002/anie.201205923.
10. A.H. Alshehri, M. Jakubowska, A. Młożniak, M. Horaczek, D. Rudka, C. Free, J.D. Carey, Enhanced Electrical Conductivity of Silver Nanoparticles for High Frequency Electronic Applications, ACS Appl. Mater. Interfaces. 4 (2012) 7007–7010. https://doi.org/10.1021/am3022569.
11. R. Ma, B. Kang, S. Cho, M. Choi, S. Baik, Extraordinarily High Conductivity of Stretchable Fibers of Polyurethane and Silver Nanoflowers, ACS Nano. 9 (2015) 10876–10886. https://doi.org/10.1021/acsnano.5b03864.
12. D. Basak, S. Karan, B. Mallik, Significant modifications in the electrical properties of poly(methyl methacrylate) thin films upon dispersion of silver nanoparticles, Solid State Commun. 141 (2007) 483–487. https://doi.org/https://doi.org/10.1016/j.ssc.2006.12.014.
13. K. Gupta, P.C. Jana, A.K. Meikap, Optical and electrical transport properties of polyaniline–silver nanocomposite, Synth. Met. 160 (2010) 1566–1573. https://doi.org/https://doi.org/10.1016/j.synthmet.2010.05.026.
14. K. Suganuma, S. Sakamoto, N. Kagami, D. Wakuda, K.-S. Kim, M. Nogi, Low-temperature low-pressure die attach with hybrid silver particle paste, Microelectron. Reliab. 52 (2012) 375–380. https://doi.org/https://doi.org/10.1016/j.microrel.2011.07.088.
15. B. Bhattarai, I. Chakraborty, B.E. Conn, A. Atnagulov, T. Pradeep, T.P. Bigioni, High-Yield Paste-Based Synthesis of Thiolate-Protected Silver Nanoparticles, J. Phys. Chem. C. 121 (2017) 10964–10970. https://doi.org/10.1021/acs.jpcc.6b12427.
16. F.S. Rosarin, S. Mirunalini, Nobel Metallic Nanoparticles with Novel Biomedical Properties, J. Bioanal. Biomed. 03 (2011) 85–91. https://doi.org/10.4172/1948-593x.1000049.
17. X. Dai, Q. Guo, Y. Zhao, P. Zhang, T. Zhang, X. Zhang, C. Li, Functional Silver Nanoparticle as a Benign Antimicrobial Agent That Eradicates Antibiotic-Resistant Bacteria and Promotes Wound Healing, ACS Appl. Mater. Interfaces. 8 (2016) 25798–25807. https://doi.org/10.1021/acsami.6b09267.
18. A. Leelavathi, T.U. Bhaskara Rao, T. Pradeep, Supported quantum clusters of silver as enhanced catalysts for reduction, Nanoscale Res. Lett. 6 (2011) 123. https://doi.org/10.1186/1556-276X-6-123.
19. D.Y. Zhang, J. Liu, Y.S. Shi, Y. Wang, H.F. Liu, Q.L. Hu, L. Su, J. Zhu, Antifouling polyimide membrane with surface-bound silver particles, J. Memb. Sci. 516 (2016) 83–93. https://doi.org/10.1016/j.memsci.2016.06.012.

20. Y. Seo, J. Hwang, J. Kim, Y. Jeong, M.P. Hwang, J. Choi, Antibacterial activity and cytotoxicity of multi-walled carbon nanotubes decorated with silver nanoparticles, Int. J. Nanomedicine. 9 (2014) 4621–4629. https://doi.org/10.2147/IJN.S69561.
21. M. Riaz, U. Sharafat, N. Zahid, M. Ismail, J. Park, B. Ahmad, N. Rashid, M. Fahim, M. Imran, A. Tabassum, Synthesis of Biogenic Silver Nanocatalyst and their Antibacterial and Organic Pollutants Reduction Ability, ACS Omega. 7 (2022) 14723–14734. https://doi.org/10.1021/acsomega.1c07365.
22. K.B. Narayanan, N. Sakthivel, Biological synthesis of metal nanoparticles by microbes, Adv. Colloid Interface Sci. 156 (2010) 1–13. https://doi.org/10.1016/j.cis.2010.02.001.
23. C. Li, Y. Xu, W. Tu, G. Chen, R. Xu, Metal-free photocatalysts for various applications in energy conversion and environmental purification, Green Chem. 19 (2017) 882–899. https://doi.org/10.1039/c6gc02856j.
24. A. Desireddy, B.E. Conn, J. Guo, B. Yoon, R.N. Barnett, B.M. Monahan, K. Kirschbaum, W.P. Griffith, R.L. Whetten, U. Landman, T.P. Bigioni, Ultrastable silver nanoparticles, Nature. 501 (2013) 399–402. https://doi.org/10.1038/nature12523.
25. P. Singh, H. Singh, Y.J. Kim, R. Mathiyalagan, C. Wang, D.C. Yang, Extracellular synthesis of silver and gold nanoparticles by Sporosarcina koreensis DC4 and their biological applications, Enzyme Microb. Technol. 86 (2016) 75–83. https://doi.org/10.1016/j.enzmictec.2016.02.005.
26. C. Li, Y. Zhang, M. Wang, Y. Zhang, G. Chen, L. Li, D. Wu, Q. Wang, In vivo real-time visualization of tissue blood flow and angiogenesis using Ag2S quantum dots in the NIR-II window, Biomaterials. 35 (2014) 393–400. https://doi.org/https://doi.org/10.1016/j.biomaterials.2013.10.010.
27. I. Sondi, B. Salopek-Sondi, Silver nanoparticles as antimicrobial agent: a case study on E. coli as a model for Gram-negative bacteria, J. Colloid Interface Sci. 275 (2004) 177–182. https://doi.org/https://doi.org/10.1016/j.jcis.2004.02.012.
28. M. De, P.S. Ghosh, V.M. Rotello, Applications of nanoparticles in biology, Adv. Mater. 20 (2008) 4225–4241. https://doi.org/10.1002/adma.200703183.
29. S.M. Radke, E.C. Alocilja, A high density microelectrode array biosensor for detection of E. coli O157:H7, Biosens. Bioelectron. 20 (2005) 1662–1667. https://doi.org/https://doi.org/10.1016/j.bios.2004.07.021.
30. S. Gurunathan, J.H. Park, J.W. Han, J. Kim, Comparative assessment of the apoptotic potential of silver nanoparticles synthesized by Bacillus tequilensis and Calocybe indica in MDA-MB-231 human breast cancer cells : targeting p53 for anticancer therapy, Int. J. Nanomedicine. 10 (2015) 4203–4223.
31. A. Khalid, A. Ibrahim, O.C.S. Al-Hamouz, T. Laoui, A. Benamor, M.A. Atieh, Fabrication of polysulfone nanocomposite membranes with silver-doped carbon nanotubes and their antifouling performance, J. Appl. Polym. Sci. 134 (2017) 1–12. https://doi.org/10.1002/app.44688.
32. Ihsanullah, T. Laoui, A.M. Al-Amer, A.B. Khalil, A. Abbas, M. Khraisheh, M.A. Atieh, Novel anti-microbial membrane for desalination pretreatment: A silver nanoparticle-doped carbon nanotube membrane, Desalination. 376 (2015) 82–93. https://doi.org/10.1016/j.desal.2015.08.017.
33. K. Page, R.G. Palgrave, I.P. Parkin, M. Wilson, S.L.P. Savin, A. V. Chadwick, Titania and silver-titania composite films on glass - Potent antimicrobial coatings, J. Mater. Chem. 17 (2007) 95–104. https://doi.org/10.1039/b611740f.
34. L.E. Rananga, T. Magadzu, Comparative studies of silver doped carbon nanotubes and β-cyclodextrin for water disinfection, Dig. J. Nanomater. Biostructures. 10 (2015) 831–836. https://doi.org/http://www.chalcogen.ro/831_Rananga.pdf.
35. A.K. Shukla, J. Alam, M.A. Ansari, M. Alhoshan, M. Alam, A. Kaushik, Selective ion removal and antibacterial activity of silver-doped multi-walled carbon nanotube / polyphenylsulfone nanocomposite membranes, Mater. Chem. Phys. 233 (2019) 102–112. https://doi.org/10.1016/j.matchemphys.2019.05.054.
36. R. Su, Y. Jin, Y. Liu, M. Tong, H. Kim, Bactericidal activity of Ag-doped multi-walled carbon nanotubes and the effects of extracellular polymeric substances and natural organic matter, Colloids Surfaces B Biointerfaces. 104 (2013) 133–139. https://doi.org/10.1016/j.colsurfb.2012.12.002.
37. A. Ohnuma, K. Iwasaki, T.B. Corporation, Development of n-type silver-nanoparticles-modi fi ed carbon materials doped by triphenylphosphine, MRS Commun. (2017) 1–5. https://doi.org/10.1557/mrc.2017.48.
38. K.M.M. Abou El-Nour, A. Eftaiha, A. Al-Warthan, R.A.A. Ammar, Synthesis and applications of silver nanoparticles, Arab. J. Chem. 3 (2010) 135–140. https://doi.org/10.1016/j.arabjc.2010.04.008.
39. V.K. Sharma, R.A. Yngard, Y. Lin, Silver nanoparticles: Green synthesis and their antimicrobial activities, Adv. Colloid Interface Sci. 145 (2009) 83–96. https://doi.org/10.1016/j.cis.2008.09.002.
40. W.H.O. (WHO), Guidelines for drinking-water quality, 4th edition, incorporating the 1st addendum, 4th ed., World Health Organization, 2017.
41. H.G. Gorchev, G. Ozolins, Guidelines for drinking-water quality, 2011. https://doi.org/10.1016/S1462-0758(00)00006-6.

42. H. Ou-Yang, G. Stamatas, N. Kollias, Spectral Responses of Melanin to Ultraviolet A Irradiation, J. Invest. Dermatol. 122 (2004) 492–496. https://doi.org/https://doi.org/10.1046/j.0022-202X.2004.22247.x.
43. M. Al Khatib, M. Harir, J. Costa, M.C. Baratto, I. Schiavo, L. Trabalzini, S. Pollini, G.M. Rossolini, R. Basosi, R. Pogni, Spectroscopic Characterization of Natural Melanin from a Streptomyces cyaneofuscatus Strain and Comparison with Melanin Enzymatically Synthesized by Tyrosinase and Laccase, Molecules. 23 (2018). https://doi.org/10.3390/molecules23081916.